GEOPHYSICS, VOL. 59, NO. 5 (MAY 1994); P. 722-732, 9 FIGS.



# The equivalent data concept applied to the interpolation of potential field data

Carlos Alberto Mendonça* and João B. C. Silva*


## ABSTRACT

The equivalent layer calculation becomes more efficient by first converting the observed potential data set to a much smaller equivalent data set, thus saving considerable CPU time. This makes the equivalent-source method of data interpolation very competitive with other traditional gridding techniques that ignore the fact that potential anomalies are harmonic functions. The equivalent data set is obtained by using a least-squares iterative algorithm at each iteration that solves an underdetermined system fitting all observations selected from previous iterations and the observation with the greatest residual in the preceding iteration. The residuals are obtained by computing a set of "predicted observations" using the estimated parameters at the current iteration and subtracting them from the observations. The use of Cholesky's decomposition to implement the algorithm leads to an efficient solution update everytime a new datum is processed. In addition, when applied to interpolation problems using equivalent layers, the method is optimized by approximating dot products by the discrete form of an analytic integration that can be evaluated with much less computational effort. Finally, the technique is applied to gravity data in a $2 \times 2$ degrees area containing 3137 observations, from Equant-2 marine gravity survey offshore northern Brazil. Only 294 equivalent data are selected and used to interpolate the anomalies, creating a regular grid by using the equivalent-layer technique.

For comparison, the interpolation using the minimum-curvature method was also obtained, producing equivalent results.

The number of equivalent observations is usually one order of magnitude smaller than the total number of observations. As a result, the saving in computer time and memory is at least two orders of magnitude as compared to interpolation by equivalent layer using all observations.


## INTRODUCTION

Some techniques for interpreting potential field data in exploration geophysics require the knowledge of anomalies on a regular grid. As measurements at regular intervals are difficult to obtain in practice, the usual procedure is to obtain the regular grid from an irregular set of observations by a process called gridding.

Aiming at simplicity of implementation, the earliest gridding processes employed inverse-of-distance weights (La Porte, 1962) or a local polynomial fitting Braile (1978). More elaborated methods using different forms of spline functions were introduced by Bhattacharyya (1969), Briggs (1974), and Enriquez et al. (1983). However, these methods assume that a potential field anomaly is a smooth function and not a harmonic function. The vertical gravity anomaly is always harmonic, but the total magnetic intensity anomaly is a harmonic function only if its magnitude is much smaller than the magnitude of the geomagnetic field, which is true for most anomalies on the earth's surface.

Both the collocation method (Moritz, 1977, 1978; Morrisson and Douglas, 1984) and the equivalent layer technique (Dampney, 1969) use harmonic interpolating functions, but their computational efficiency rapidly degrades as the amount of data increases. A particular situation occurs when the data set is large but the anomaly is very smooth, as is the case of satellite magnetic data. In this case, a few sources can be used to fit all data, and the equivalent-layer problem is solved by an overdetermined formulation (Mayhew et al., 1980). However, this approach is less efficient when applied to a general situation in which potential field data are not

Manuscript received by the Editor November 2, 1992; revised manuscript received August 10, 1993.
*CG-UFPA-Caixa Postal 1611, 66017-900-Belem-PA, Brazil

sufficiently smooth, such as in standard aeromagnetic surveys.

The iterative residual modeling methods used by von Frese et al. (1988) and Cordell (1992) do not guarantee convergence because at each iteration they solve an overdetermined problem, fitting all data by using just a few or even only one equivalent source. On the other hand, convergence is guaranteed if an underdetermined problem is solved at each iteration (van der Sluis and van der Vorst, 1987; Ladas and Devaney, 1991).

We present an operational interpolation technique that introduces the constraint that the interpolating function must satisfy Laplace's equation using the equivalent-layer technique. The equivalent-layer technique has been used widely in the literature (Bott, 1967; Bott and Ingles, 1972; Dampney, 1969; Emilia, 1973; von Frese et al., 1981; Silva, 1986), and there are efficient algorithms to solve equivalent-layer problems associated with large sets of gridded data (Leão and Silva, 1989). To apply the equivalent-layer technique to interpolation problems, however, we must obtain, from randomly positioned observations, the intensities of the linear parameters (density or dipole moment) of the equivalent sources usually situated at a constant depth. In this case, it is often necessary to solve a linear system with size equal to the number of data (usually of the order of thousands) or equal to the number of linear parameters (which must be close to the number of data to produce a good fit). This, therefore, restricts the current random-to-grid operations using the equivalent-layer technique to small data sets (order of hundreds) because of limitations in memory and CPU time of today's computers.

To overcome this difficulty, we developed the concept of equivalent data: a subset of all observations such that an interpolating function, derived from the equivalent-layer principle, which fits the subset of observations will also fit the remaining observations. The number of equivalent observations will depend on the roughness of the anomaly surface. Because the occurrence of smooth potential field anomalies is not uncommon, the number of equivalent data may be substantially smaller than the total number of data, which makes the equivalent-layer technique a feasible interpolation method.

## THE EQUIVALENT-LAYER TECHNIQUE

By the equivalent-layer principle, the potential field observations can be written as

$$\mathbf{d} = \underline{\mathbf{G}}\mathbf{p}, \tag{1}$$

where $\mathbf{d}$ is a vector with $N$ observations, $\mathbf{p}$ is a vector with $M$ unknown intensities of the equivalent sources, and $\underline{\mathbf{G}}$ is an $N \times M$ kernel matrix that maps the sources to data. The element $g_{n,m}$ of $\underline{\mathbf{G}}$ is written as

$$g_{n,m} = g(x_n - x_m,\ y_n - y_m,\ z_n - h) \tag{2}$$

and at the $n$th observation location $(x_n, y_n, z_n)$, represents a quantity proportional to the effect of the $m$th equivalent source situated at $(x_m, y_m, h)$.

We formulate the equivalent-layer problem given in equation (1) in an underdetermined way, by assuming a number of equivalent sources greater than the number of observations. As compared to an overdetermined formulation, this formulation yields smaller residuals between the observations and their representations in equation (1) which is a very important requirement for an interpolation method.

Formulated as an underdetermined problem, equation (1) does not have an unique solution. Therefore, we look for the solution that has the minimum Euclidean norm. As the data are corrupted with noise, we use a damping factor, $\lambda > 0$ (Silva, 1986) to obtain the estimator $\hat{\mathbf{p}}$ as

$$\hat{\mathbf{p}} = \underline{\mathbf{G}}^T\mathbf{w}, \tag{3}$$

where vector $\mathbf{w}$ is a dummy variable obtained by solving the linear system

$$\underline{\mathbf{D}}^{-1}(\underline{\mathbf{D}}\underline{\mathbf{G}}\underline{\mathbf{G}}^T\underline{\mathbf{D}} + \lambda\underline{\mathbf{I}})\underline{\mathbf{D}}^{-1}\mathbf{w} = \mathbf{d}, \tag{4}$$

where $\underline{\mathbf{I}}$ is an $N \times N$ identity matrix and $\underline{\mathbf{D}}$ is a diagonal normalizing matrix with elements:

$$d_{n,n} = \left[\sum_{m=1}^{M} g_{n,m}^2\right]^{-1/2}, \qquad n = 1, \ldots, N. \tag{5}$$

The purpose of normalization is to constrain the practical range of $\lambda$ to the interval [0, 1]. This normalizing procedure is used in all matrix operations involving parameter $\lambda$; however, to keep the notation simple, the normalizing operation will be omitted in the text.

The equivalent sources estimate $\hat{\mathbf{p}}$ provides an analytic harmonic function of the form

$$d(x, y, z) = \sum_{m=1}^{M} g(x - x_m, y - y_m, z - h)\hat{p}_m \tag{6}$$

that fits all observations if $\lambda$ is equal to zero. When the data are corrupted with noise, an exact fit is not desirable. In this case, a value of $\lambda$ greater than zero should be selected to produce misfits of the order of the noise amplitude in data. The interpolated value $d_k$, at position $(x_k, y_k, z_k)$, is evaluated by equation (6) and can be written as a dot product

$$d_k = \mathbf{g}_{(k)}^T\hat{\mathbf{p}}, \tag{7}$$

or, using equation (3), as

$$d_k = \mathbf{g}_{(k)}^T\underline{\mathbf{G}}^T\mathbf{w}, \tag{8}$$

where $\mathbf{g}_{(k)}$ is a vector whose $i$th element is $g(x_k - x_i, y_k - y_i, z_k - h)$. The random-to-grid operation is realized by evaluating equation (7) or (8) for a set of positions $k$ situated on a regular grid.

Theoretically, the equivalent layer does not have to be at a constant depth. However, assuming equivalent layers at different depths will degrade the method's efficiency and make it less operational, because the user will have to decide about the depth of the equivalent layer within each subarea corresponding to different subsets of the whole set of observations. The (constant) depth of the equivalent layer should not be smaller than 2.5 times the spacing between data points, otherwise aliasing may occur (Dampney, 1969). Particularly, in aeromagnetic and marine surveys, where the spacing between flight lines and ship tracks, respectively,

may be substantially greater than the spacing between stations along a flight line (or track), the use of a shallow equivalent layer will produce aliasing in the interpolated data in the direction perpendicular to the flight lines (or tracks).

Unfortunately, this formulation of the equivalent-layer technique cannot be used for large data sets because of two difficulties. The first one is the tremendous computational effort required for the evaluation of matrix product $\underline{G}\underline{G}^T$ because each one of its elements is a dot product requiring $M$ multiplications. The second difficulty is the huge storage and the excessive CPU time required for solving the linear system given in equation (4) because of the large dimension of matrix $\underline{G}\underline{G}^T$, dictated by the large number of data present in a survey.

To overcome both difficulties, we developed two methods. The first one optimizes the evaluation of the dot products interpreting it as a discrete integration with a known closed-form solution that can be evaluated with much less computational effort. The second method is based on the concept of equivalent data and chooses a subset of all data points, such that the interpolating surface that fits the chosen subset also automatically fits all remaining data points. Both approaches are described below and are efficient tools for solving equivalent-layer problems associated with large data sets.

## THE OPTIMIZED DOT PRODUCT EVALUATION

The entry $i, j$ of matrix $\underline{G}\underline{G}^T$ is the dot product

$$\mathbf{g}_{(i)}^T\mathbf{g}_{(j)} = \sum_{m=1}^{M} g(x_m - x_i,\ y_m - y_i,\ z_i - h) \cdot g(x_m - x_j,\ y_m - y_j,\ z_j - h), \quad (9)$$

where vector $\mathbf{g}_{(k)}$ is the $k$th row of matrix $\underline{G}$. Each entry requires $M$ multiplications and, as $\underline{G}\underline{G}^T$ is a symmetric matrix, the computation of the entire matrix needs $N(N+1)M/2$ multiplications. By renumbering the sources assumed to be distributed on an $M_x \times M_y$ rectangular grid, we can write

$$\mathbf{g}_{(i)}^T\mathbf{g}_{(j)} = \sum_{i_y=1}^{M_y}\sum_{i_x=1}^{M_x} g(x_\ell - x_i,\ y_\ell - y_i,\ z_i - h) \cdot g(x_\ell - x_j,\ y_\ell - y_j,\ z_j - h), \quad (10)$$

where $\ell = M_x(i_y - 1) + i_x$. By multiplying both terms of equation (10) by $\Delta x \cdot \Delta y$ (respectively, the distances between adjacent sources in the $x$ and $y$ directions), the right-hand side term can be interpreted as a discrete integration of

$$\int_{-\infty}^{+\infty}\int_{-\infty}^{+\infty} g(\alpha - x_i,\ \beta - y_i,\ z_i - h) \cdot g(\alpha - x_j,\ \beta - y_j,\ z_j - h)\, d\alpha\, d\beta \quad (11)$$

that has an analytic solution of the form $f(x_j - x_i,\ y_j - y_i,\ 2h - z_j - z_i)$, if $g$ is a harmonic function of the inverse of distance. The analytic solution of integral (11) for a point mass is presented in the Appendix. The evaluation can be done, analogously, for a magnetic dipole, but the mathematical expression involved is much more complex.

Then the inner product (9) can be approximated by the analytic solution $f$:

$$\mathbf{g}_{(i)}^T\mathbf{g}_{(j)} \approx \frac{1}{\Delta x \Delta y} f(x_j - x_i,\ y_j - y_i,\ 2h - z_j - z_i). \quad (12)$$

For a point mass, the evaluation of equation (12) requires only seven multiplications plus one square root, while the evaluation of equation (10) needs $M$ multiplications. For a $50 \times 50$ source grid, for example, we will have $M = 2500$, while the number of operations to evaluate equation (12) remains as seven.

Using equation (12), we replace $\underline{G}\underline{G}^T$ by a matrix $\underline{F}$ whose element $f_{i,j}$ is given by

$$f_{i,j} = f(x_j - x_i,\ y_j - y_i,\ 2h - z_j - z_i)/\Delta x \Delta y. \quad (13)$$

In the same way, we replace the product $\mathbf{g}_{(k)}^T\underline{G}^T$ in equation (8) by the vector $\mathbf{f}_{(k)}$ whose $i$th element is given by $f(x_i - x_k,\ y_i - y_k,\ 2h - z_i - z_k)/\Delta x \Delta y$, yielding

$$d_k = \mathbf{f}_{(k)}^T\mathbf{w}, \quad (14)$$

where vector $\mathbf{w}$ is obtained by solving the linear system

$$(\underline{F} + \lambda'\underline{I})\mathbf{w} = \mathbf{d} \quad (15)$$

with $\lambda' = \Delta x \Delta y \lambda$.

For $\lambda'$ equal to zero, the interpolated observation is written as

$$d_k = \mathbf{f}_{(k)}^T\underline{F}^{-1}\mathbf{d}, \quad (16)$$

which is the same as the matrix formulation of the collocation problems (Moritz, 1977). In this case the function $f$ has the meaning of a covariance function.

## THE EQUIVALENT DATA CONCEPT

The concept of equivalent data is based on the assumption that there is an integer $e \leq M$ such that when the linear system given in equation (1) is split as

$$\begin{bmatrix}\mathbf{d}_e\\ \mathbf{d}_r\end{bmatrix} = \begin{pmatrix}\underline{G}_e\\ \underline{G}_r\end{pmatrix}\mathbf{p}, \quad (17)$$

the estimates using only data $\mathbf{d}_e$

$$\hat{\mathbf{p}}_e = \underline{G}_e^T(\underline{G}_e\underline{G}_e^T + \lambda\underline{I})^{-1}\mathbf{d}_e, \quad (18)$$

yield a residual vector

$$\mathbf{r} = \mathbf{d}_r - \underline{G}_r\hat{\mathbf{p}}_e, \quad (19)$$

whose Chebychev norm (the greatest vector element in absolute value) is equal to or smaller than a predetermined value $\mathscr{C}$ related to the maximum expected error in observations.

In equations (17)–(19), $\underline{G}_e$ and $\underline{G}_r$ are, respectively, $e \times M$ and $r \times M$ matrices and $\mathbf{d}_e$ and $\mathbf{d}_r$ are vectors belonging to the $e$- and $r$-dimensional spaces, respectively. Note that the estimator $\hat{\mathbf{p}}_e$ in equation (18) is obtained using only the data vector $\mathbf{d}_e$. For this reason it is called the equivalent data vector while $\mathbf{d}_r$ is called the redundant data vector.

To obtain the equivalent data related to a linear system, we developed the iterative algorithm, called determination of equivalent data (DED), with the following five steps:

1) Identify the largest element of vector $\mathbf{d}$ in absolute value. This is the first equivalent datum while, for the moment, all remaining elements are considered as redundant data.
2) Using only the $n$ current equivalent data, compute the solution vector $\hat{\mathbf{p}}_n$ as given in equation (18).
3) Evaluate the residuals $r_k = d_k - \mathbf{g}_{(k)}^T \hat{\mathbf{p}}_n$ for all current redundant data, that is, for $k = n + 1, n + 2, \ldots, N$.
4) Find the datum $d_q$ associated with the greatest absolute residual $r_q$.
5) If the residual $r_q$ is greater than the predetermined value $\mathcal{C}$, accept $d_q$ as a new equivalent datum, increase $n$ by one and go to step 2. If the residual is smaller than $\mathcal{C}$, make $e = n$ and stop the iteration.

The DED algorithm works even in the case $e = N$ when the whole data set is selected as equivalent data.

DED is an iterative algorithm that includes one additional datum (one matrix row) every time step (2) is executed. This feature makes DED a new type of algebraic reconstruction technique (ART) algorithm (Tarantola, 1987; van der Sluis and van der Vorst, 1987). In traditional ART algorithms, the rows are processed sequentially while, in the DED algorithm, the rows are introduced according to their residual magnitudes computed from the estimates of $\mathbf{p}_e$ in the preceding iteration.

The Chebychev norm is used to ensure that the fit at each redundant data point produces a residual equal to or smaller than $\mathcal{C}$. At equivalent data, however, this quality of fit is not guaranteed. For example, if a particular observation is corrupted with high-amplitude, high-frequency noise, it will probably become an equivalent observation because the residual at this observation will probably become the largest one in absolute value. Therefore, the most noisy data are prone to become equivalent observations. Moreover, depending on the trade-off between noise amplitude (and frequency) and the depth of the equivalent layer, the residuals at equivalent observations cannot be made smaller than $\mathcal{C}$ as desired. The use of the Chebychev norm also makes the method less sensitive to the choice of $\mathcal{C}$ because it places an upper bound on the absolute value of residuals at redundant observations. Consequently, small changes in this bound will not change the interpolating surface substantially at these points. At equivalent points, where the residuals may exceed $\mathcal{C}$, substantial changes might occur. However, the percentage of points with large residuals is necessarily small, otherwise the interpolation would be meaningless.

The equivalent data are defined in association with a generic linear system and may have several interpretations. In the equivalent-layer problem, for example, vector $\mathbf{d}$ defines all data points belonging to an anomaly surface, and the equivalent data $\mathbf{d}_e$ consist of selected data points such that the interpolating surface that fits these data points will automatically fit all the remaining data points $\mathbf{d}_r$. This geometric interpretation of equivalent data holds for any data that may be represented by a surface like topography, for example. For tomography problems, on the other hand, the equivalent data are related to the complexity of the media. For homogeneous and isotropic media, for example, the number of equivalent data is one because the slowness that reproduces one traveltime will reproduce any other observed traveltime.

## THE DED ALGORITHM COMPUTATIONAL IMPLEMENTATION

To reduce computational effort, the implementation of the DED algorithm must use matrix relationships that allow an update of the solution everytime a new row is processed in the same way as in ART algorithms. However, the current ART algorithms are suitable for dealing with sparse matrices but not with full matrices as in equivalent-layer problems. In this section we present a DED computational implementation that updates the solution using intrinsic properties of Cholesky's decomposition.

Using the matrix relationship given by equation (14), the $n$th iteration of DED involves the evaluation of the interpolating surface by

$$d_k = \mathbf{w}_n^T \mathbf{f}_n^k, \tag{20}$$

where $\mathbf{w}_n$ is obtained by solving the system

$$(\underline{\mathbf{F}}_n + \lambda' \underline{\mathbf{I}})\mathbf{w}_n = \mathbf{d}_n. \tag{21}$$

The subscripts now denote the dimensions of vectors and square matrices to make it clear that, for every processed datum, the dimension of the linear system increases by one.

In the same way, we have for the $(n + 1)$st iteration:

$$d_k = \mathbf{w}_{n+1}^T \mathbf{f}_{n+1}^k, \tag{22}$$

where $\mathbf{w}_{n+1}$ is obtained by solving the system

$$(\underline{\mathbf{F}}_{n+1} + \lambda' \underline{\mathbf{I}})\mathbf{w}_{n+1} = \mathbf{d}_{n+1}, \tag{23}$$

where

$$\mathbf{f}_{n+1}^k = \begin{bmatrix} \mathbf{f}_n^k \\ f_{k,n+1} \end{bmatrix}, \qquad \underline{\mathbf{F}}_{n+1} = \begin{pmatrix} \underline{\mathbf{F}}_n & \mathbf{h}_n \\ \mathbf{h}_n^T & f_{n+1,n+1} \end{pmatrix}, \qquad \mathbf{d}_{(n+1)} = \begin{bmatrix} \mathbf{d}_n \\ d_{n+1} \end{bmatrix} \tag{24}$$

and

$$\mathbf{h}_n^T = [f_{1,n+1} \; f_{2,n+1} \cdots f_{n,n+1}]. \tag{25}$$

As the linear systems given in equations (21) and (23) involve symmetric, positive-definite matrices (for positive $\lambda'$), they can be solved through the Cholesky's decomposition of these matrices:

$$\underline{\mathbf{C}}_n \underline{\mathbf{C}}_n^T = (\underline{\mathbf{F}}_n + \lambda' \underline{\mathbf{I}}) \tag{26}$$

for the system in equation (21) and

$$\underline{\mathbf{C}}_{n+1} \underline{\mathbf{C}}_{n+1}^T = (\underline{\mathbf{F}}_{n+1} + \lambda' \underline{\mathbf{I}}) \tag{27}$$

for the system in equation (23). Solutions $\mathbf{w}_n$ and $\mathbf{w}_{n+1}$ are obtained by applying the forward and backward substitution (Tarantola, 1987).

To obtain $\underline{\mathbf{C}}_{n+1}$ we just border matrix $\underline{\mathbf{C}}_n$ as

$$\underline{C}_{n+1} = \begin{pmatrix} \underline{C}_n & \mathbf{0} \\ \mathbf{c}_n^T & c_{n+1} \end{pmatrix}, \tag{28}$$

where the $i$th element $c_i^n$ of vector $\mathbf{c}_n$ is given by

$$c_i^n = \left( h_i^n - \sum_{m=1}^{i-1} c_{i,m} c_{n,m} \right) \Big/ c_{i,i}, \tag{29}$$

where $h_i^n$ is the $i$th element of vector $\mathbf{h}_n$ and the diagonal entry $c_{n+1}$ is given by

$$c_{n+1} = \left( f_{(n+1,n+1)} + \lambda' - \sum_{k=1}^{n-1} c_{n+1,k}^2 \right)^{1/2}. \tag{30}$$

Equations (29) and (30) arise from the very definition of Cholesky's decomposition (Tarantola, 1987).

Figure 1 shows the number of floating point operations required to solve the linear system (21), using the above described computational implementation, as a function of the number $n$ of equivalent observations for an original set of 1000 observations. For the purpose of comparison, we also include the number of operations required to solve the linear system (15) for $N = 1000$ (using Cholesky's decomposition of the entire matrix $\underline{F} + \lambda'\underline{I}$). The number of operations in this case is, therefore, independent of the number of equivalent observations and will be constant for a constant $N$. Note that the number of operations required by the DED algorithm reduces drastically for $n \leq 300$. For $n$ greater than about 470, DED becomes less efficient than solving the whole system. In general, DED will be more efficient when the number of equivalent observations is substantially smaller than the total number of observations.

## APPLICATION OF DED ALGORITHM TO THE INTERPOLATION OF SYNTHETIC PROFILE DATA

In this example, we use a synthetic, total intensity anomaly profile along the magnetic north azimuth, sampled at 200 points, produced by three magnetic prisms finite in the $x$ and $z$ directions and infinite in the $y$ direction (perpendicular to the plane of Figure 2). The magnetization inclination and declination of all prisms are 45 and zero degrees, respectively. The magnetization intensity is 1 A/m. The prism is magnetized only by induction. We choose a profile to illustrate the application to synthetic data because it reveals and appraises the way DED works at each iteration. Figures 3a, 3b, and 3c show the result of the second, third and fourth DED iteration, respectively, assuming $\mathscr{C} = 1$ nT. Note that, at each iteration, the algorithm produces an exact fit at the point where the greatest residual occurs in the preceding iteration, while at the same time keeping the exact fit at all previously selected equivalent points. Figure 3d shows the result of the last iteration. At completion, DED selects only 17 data points, such that the interpolating surface fitting these selected data also fits all remaining 183 data. As the data are noise-free, we use $\lambda' = 0$ to yield an exact fit. Note that DED acts as an adaptive decimation procedure.

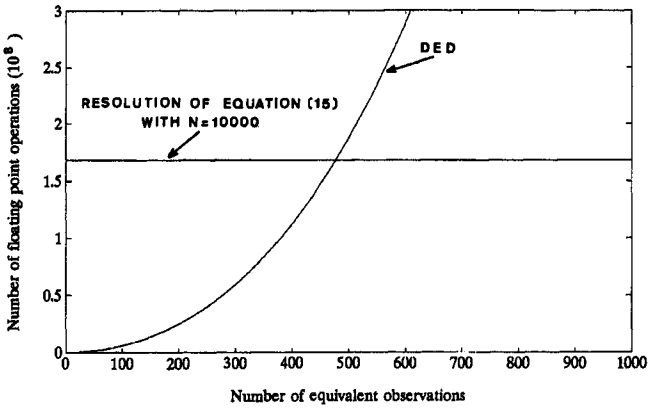


FIG. 1. Comparison between the number of floating point operations required by solving system (15) using Cholesky's decomposition of the entire 1000 × 1000 system and by the DED algorithm implemented by updating the decomposed matrix. The total number of observations is 1000 in both cases.

## APPLICATION OF DED TO INTERPOLATE REAL DATA

Figure 4 shows a 2 × 2 degree area containing the location of 3137 data points, which are part of the marine gravity data of Equant-2 survey, carried out at the Amazon River mouth offshore northern Brazil.

We applied DED to the free-air anomalies obtained at these points, using one equivalent layer situated at a depth of 10 km. The values of $\lambda'$ and $\mathscr{C}$ used were 0.01 and 3 mGal, respectively. They were chosen because they allow misfits of the order of 3 mGal which is the overall estimated data precision (Ness et al., 1989). By applying DED, we found 294 equivalent data points. From the interpolating surface

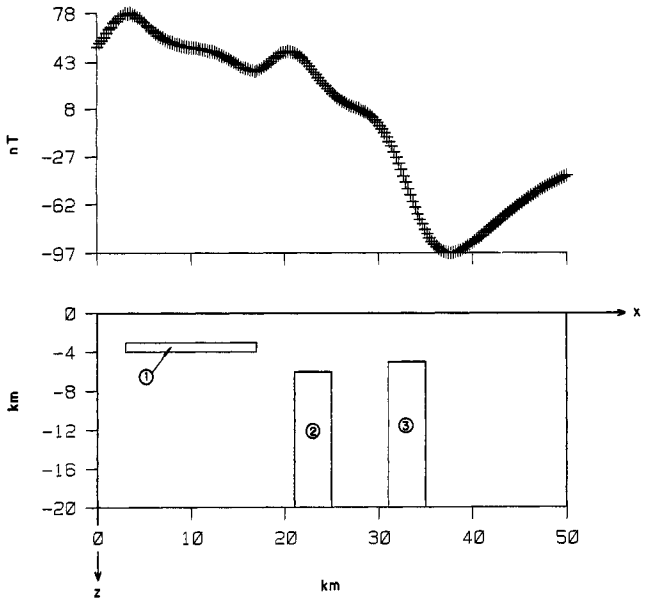


FIG. 2. Magnetic source model producing the synthetic total intensity anomaly profile along the magnetic north azimuth used to illustrate the DED algorithm. All prisms are magnetized by induction only. The inducing field has inclination and declination equal to 45 and zero degrees, respectively. Prisms 2 and 3 have infinite depth extent.

that fits the equivalent data, we evaluated the residual vector for all data points. This vector has a quadratic norm (square root of the sum of squared elements) equal to 65.84 mGal and a root-mean-square equal to 1.18 mGal. The greatest residual values at equivalent and redundant data points are 5.4 and 2.9 mGal, respectively. The maximum value of 5.4 mGal at an equivalent data point is because the equivalent layer is too deep compared to the sample interval along track. However, it cannot be placed at shallower depths because there would be a conspicuous aliasing of the interpolated data in the direction perpendicular to the tracks. The maximum residual value of 5.4 mGal, although high compared with the data precision, occurs at an isolated point. To give an idea of the significance of the residuals for the whole area, we show in Figure 5 the cumulative curve for the residuals. Observe that more than 99 percent of the absolute values of residuals are smaller than 3 mGal.

The whole interpolation process took 39 minutes of CPU time on a VAX 8600 computer. Figure 6 shows the positions of the equivalent data. From the analytic interpolating surface we evaluated equation (14) for a set of points on a regular grid, and then drew the isovalues lines of the interpolated free-air anomalies shown in Figure 7.

For the purpose of comparison, Figure 8 shows the interpolation produced with the minimum curvature method (Briggs, 1974). Both methods produced similar results.

To illustrate the aliasing effect mentioned above, in Figure 9 we show the interpolation obtained with an equivalent layer at depth of 7.5 km.

## CONCLUSIONS

The concept of equivalent data and its determination using the proposed DED algorithm are effective tools for solving

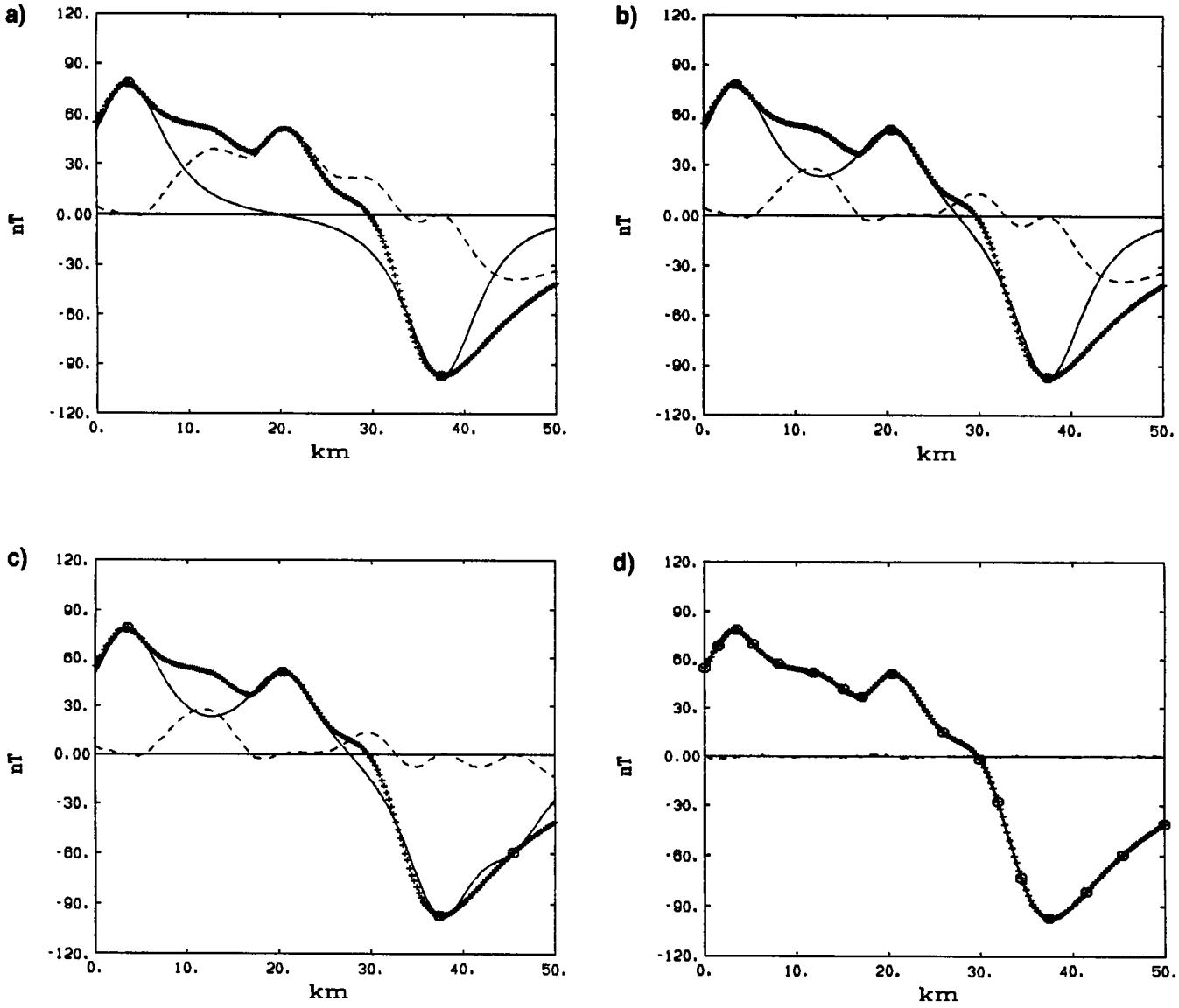


FIG. 3. (a) Second iteration of DED algorithm. The extreme values (circles) of the data vector (crosses) are fitted by an interpolating surface (solid line), and the residuals (dashed line) are the difference between the data vector and the interpolating surface; (b) third iteration; (c) fourth iteration; (d) last iteration of DED. Seventeen equivalent data were selected out of the 200 original data points.

large linear systems. By applying them, we solved an equivalent-layer problem that, by a traditional approach, would have been an impossible task on most of today's computers. However, these tools are still constrained by the number of equivalent data allowed so that it does not lead to systems that exceed the computer storage capacity. In our test with real data, we could not apply DED over the whole survey area because the number of equivalent data would be about 3000 (from a total of 19 047 observations). However, its application inside a 2 × 2 degree square was feasible because the equivalent observations were reduced to 294.

The DED algorithm processes a datum at each iteration, being then a new type of ART algorithm. Therefore, we can apply DED wherever ART is applicable (e.g., acoustical tomography) without a lot of changes in the program codes. The basic difference is that DED selects the new row corresponding to the datum to be processed according to an objective criterion, while ART processes the rows in a sequential way. DED demands, therefore, an extra computational time to sort the observations. Our algorithm may be faster than ART if the number of equivalent data is substantially smaller than the number of original data, compensating the extra time expended in the sorting. The probability that this situation will occur depends on the spatial smoothness of the observations.

The computational implementation of ART and DED algorithms must be made using matrix relationships that allow updating the solution everytime a new row is processed. For systems with full matrices, as in equivalent-layer problems, we cannot use the matrix relationships used by current ART algorithms because they are suitable for only sparse matrices. For full matrices, we developed an efficient updating procedure using the properties of Cholesky's decomposition. To avoid the expensive computation of dot products for full matrices, we first approximated the dot product to be a discrete integration that has an analytic expression. Evaluation of this analytic expression involves much less computational effort than does the original dot product.

(*Text continues on p. 731*)

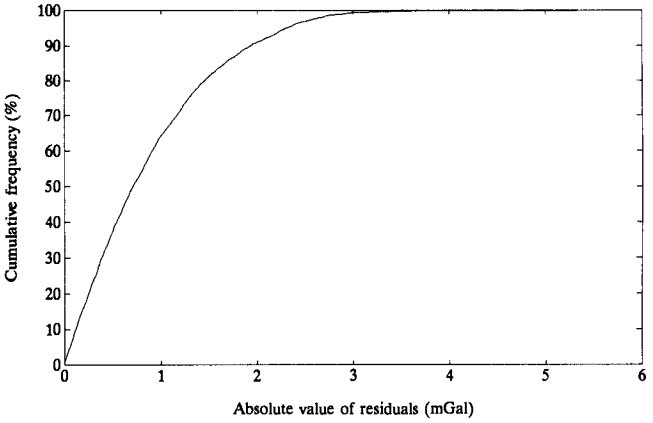


FIG. 5. Cumulative curve for the residuals computed for the 3137 data points from part of Equant-2 survey.

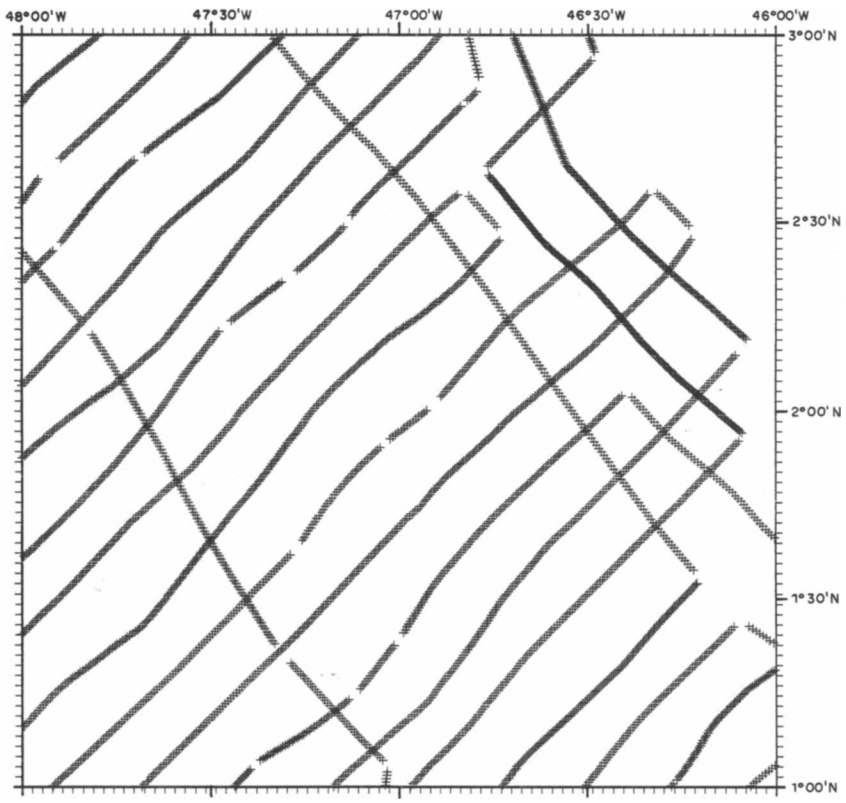


FIG. 4. Part of Equant-2 survey in a 2 × 2 degree area containing 3137 marine gravity data points (crosses).

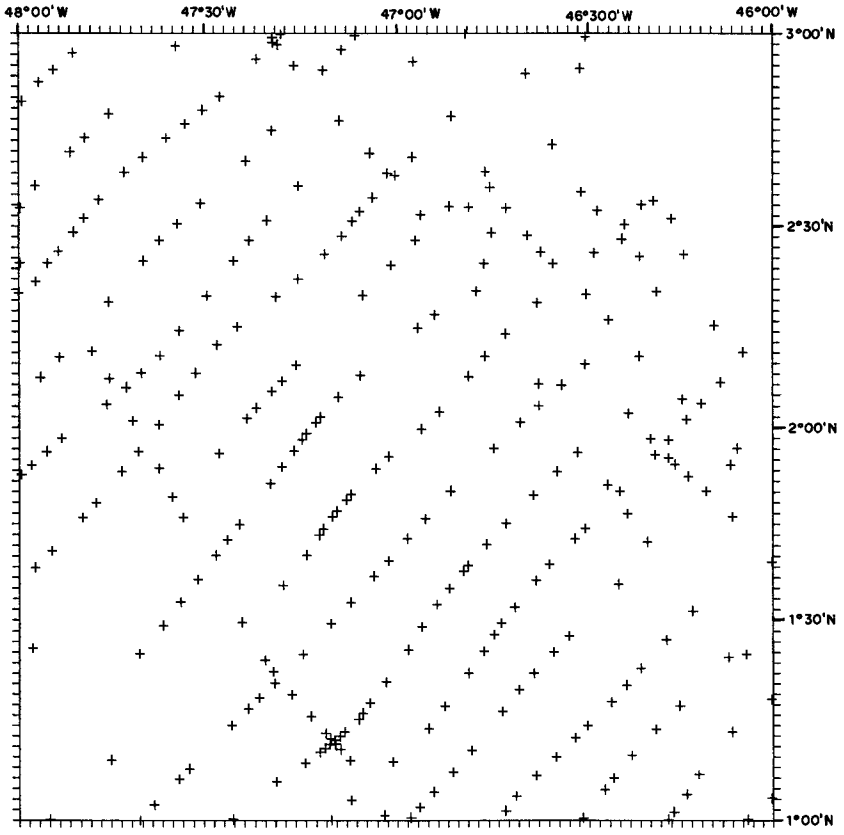


FIG. 6. Part of Equant-2 survey. Positions of the 294 equivalent data points (crosses) selected by DED from all the data points in Figure 4.

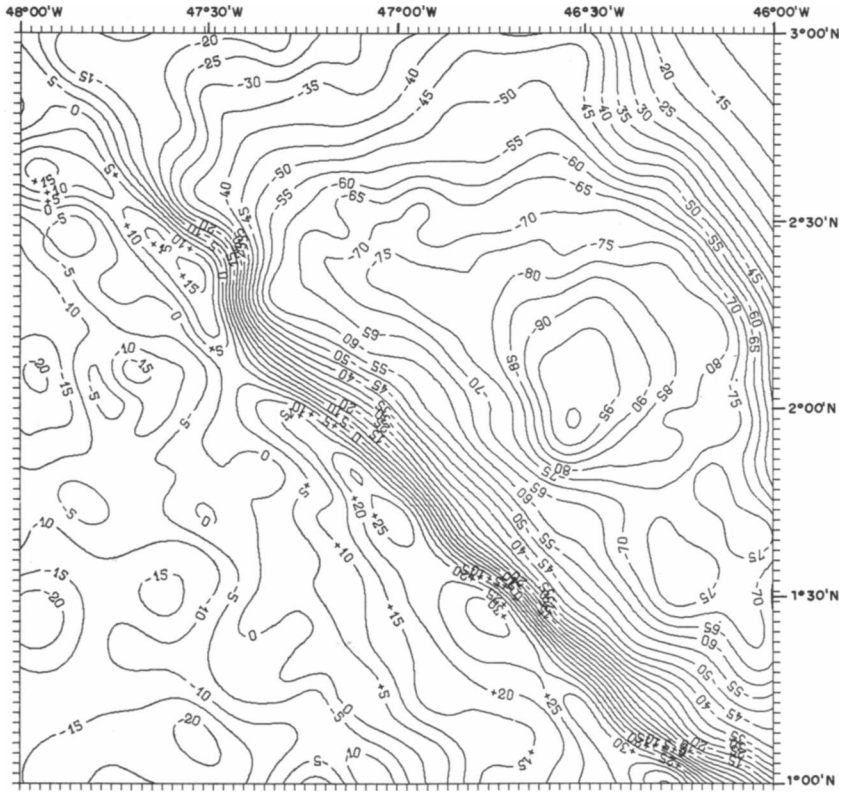


FIG. 7. Part of Equant-2 survey. Contour map of the interpolating surface obtained using the equivalent data in Figure 6 using an equivalent layer at 10 km. Contour interval is 5 mGal.

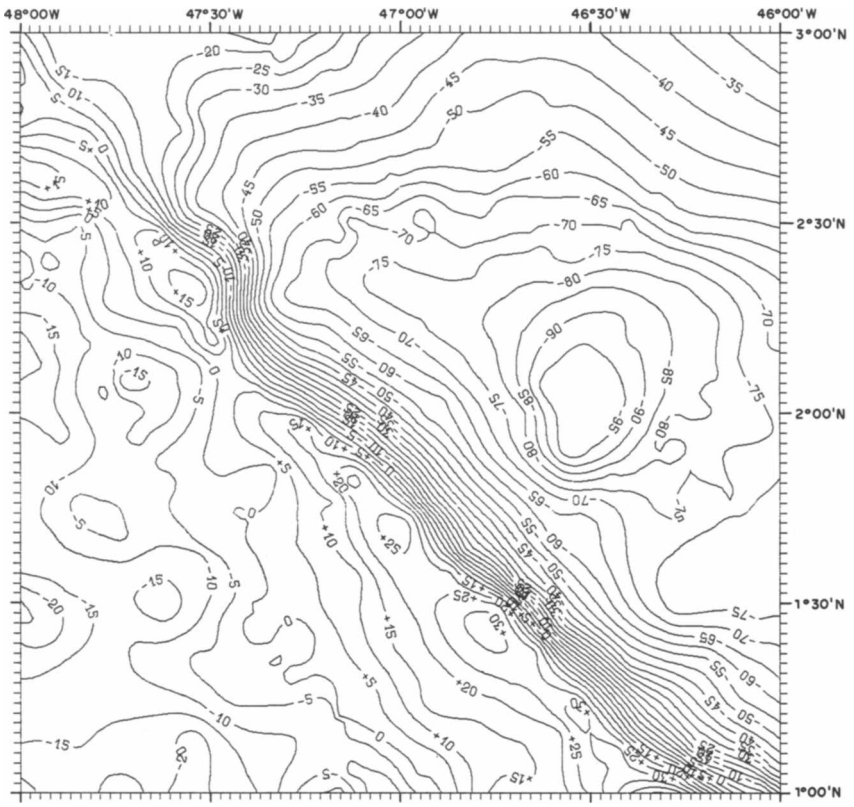


FIG. 8. Part of Equant-2 survey. Contour map of the interpolating surface obtained using the minimum-curvature method. Contour interval is 5 mGal.

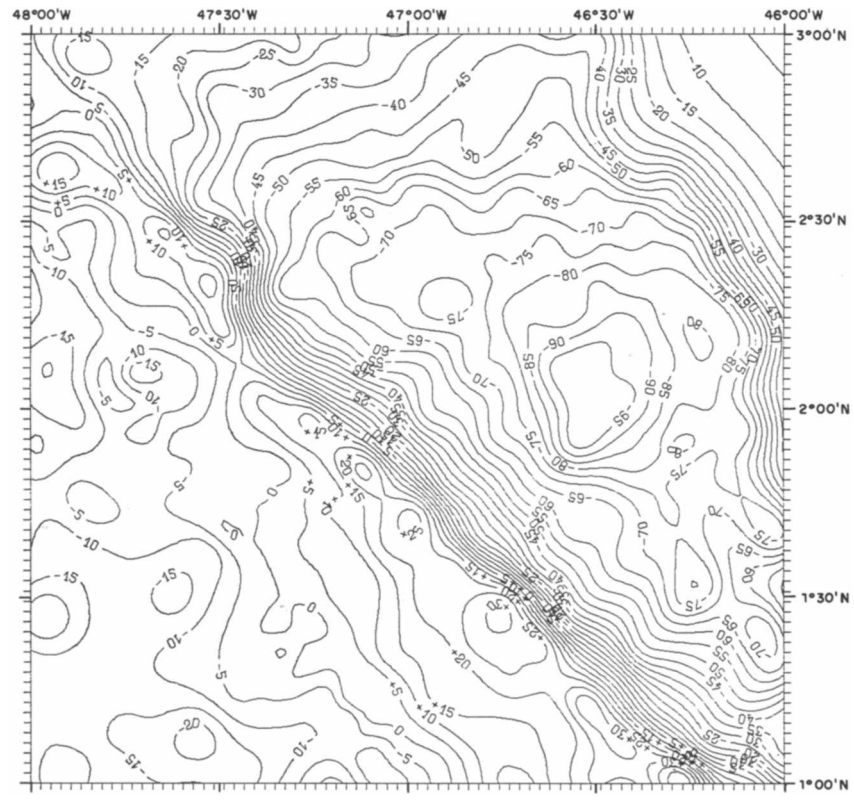


FIG. 9. Part of Equant-2 survey. Contour map of the interpolating surface using an equivalent layer at 7.5 km. Contour interval is 5 mGal.

The present method and the minimum curvature method produced similar results in the test with real data presented, but DED is more expensive than the minimum-curvature method. However, its implementation in local interpolation mode (using moving windows) would possibly make it competitive (in CPU time demand) with the minimum-curvature method. Besides, when applied to the interpolation of potential field data, DED is potentially capable of recovering undersampled anomaly amplitudes and gradients in a better manner than the minimum-curvature method because it constrains the interpolating function to be harmonic. Moreover, as far as the equivalent source intensities are computed, any processing such as reduction of data observed at different heights to a common level, derivatives, analytic continuation, etc., can be obtained simultaneously with the interpolating procedure. As a concrete advantage, DED, different from the minimum-curvature method, allows the computation of residuals between the interpolating surface and the original observations, providing an additional assessment of the interpolation quality.

The application of DED produces an analytic surface defined by $e$-basis functions that fits all data points while solving the traditional equivalent-layer problem to yield an analytic surface with $N$ basis functions. This means that DED automatically finds the smallest number of basis functions for a selected class of base of functions that will describe the data within the desired precision established by the values assigned to $\lambda'$ and $\mathcal{C}$. This fact is useful in improving the computational implementation of collocation algorithms when applied to the representation of the earth's gravity field.

## ACKNOWLEDGMENTS

We thank Núcleo de Pesquisas em Geofísica de Petróleo (NPGP) and Conselho Nacional de Desenvolvimento Científico e Tecnológico (CNPq) for supporting this research.

## REFERENCES

Bhattacharyya, B. K., 1969, Bicubic spline interpolation as a method for treatment of potential field data: Geophysics, **34**, 402–423.

Bott, M. H. P., 1967, Solution of the linear inverse problem in magnetic interpretation with application to oceanic magnetic anomalies: Geophys. J. Roy. Astr. Soc., **13**, 313–323.

Bott, M. H. P., and Ingles, A., 1972, Matrix methods for joint interpretation of two-dimensional gravity and magnetic anomalies with application to the Iceland-Faeroe Ridge: Geophys. J. Roy. Astr. Soc., **30**, 55–67.

Braile, L. W., 1978, Comparison of four random to grid methods: Computers & Geosciences, **4**, 341–349.

Briggs, I. C., 1974, Machine contouring using minimum curvature: Geophysics, **39**, 39–48.

Cordell, L., 1992, A scattered equivalent-source method for interpolation and gridding of potential-field data in three dimensions: Geophysics, **57**, 629–636.

Dampney, C. N. G., 1969, The equivalent source technique: Geophysics, **34**, 39–53.

Emilia, D. A., 1973, Equivalent sources used as an analytic base for processing total magnetic field profiles: Geophysics, **38**, 339–348.

Enriquez, J. O. C., Thomann, J., and Goupillot, M., 1983, Applications of bidimensional spline functions to geophysics: Geophysics, **48**, 1269–1273.

Ladas, K. T., and Devaney, A. J., 1991, Generalized ART algorithm for diffraction tomography: Inverse Problems, **7**, 109–125.

La Porte, M., 1962, Elaboration rapide de cartes gravimetriques deduites de l'anomalie de Bouguer a l'aide d'une calculatrice electronique: Geophys. Prosp., **10**, 238–257.

Leão, J. W. D., and Silva, J. B. C., 1989, Discrete linear transformations of potential-field data: Geophysics, **54**, 497–507.

Mayhew, M. A., Johnson, B. D., and Langel, R. A., 1980, An equivalent source model of the satellite-altitude magnetic anomaly field over Australia: Earth Plan. Sci. Lett., **51**, 189–198.

Morrisson, F. F., and Douglas, B. C., 1984, A comparison of gravity prediction methods on actual and simulated data: Geophysics, **49**, 1774–1780.

Moritz, H., 1977, Least-squares collocation and the gravitational inverse problem: J. Geophys., **43**, 153–162.

———, 1978, Least-squares collocation: Rev. Geophys. Space Phys., **16**, 421–430.

Ness, G. E., Boa Hora, M. P., Latgé, M. A., and Braga, L. F., 1989, Project Equant: A gravity and magnetic study of the northern continental margin of Brasil: 1st Congress of Brazil Geophys. Soc., Expanded Abstracts, 821–824.

Silva, J. B. C., 1986, Reduction to the pole as an inverse problem and its application to low-latitude anomalies: Geophysics, **51**, 369–382.

Tarantola, A., 1987, Inverse problem theory: Elsevier Science Publ.

van der Sluis, A., and van der Vorst, H. A., 1987, Numerical solution of large, sparse linear algebraic systems arising from tomographic problems, *in* Nolet, G., Ed., Seismic Tomography: D. Reidel Publ., 49–83.

von Frese, R. R. B., Hinze, W. J., and Braile, L. W., 1981, Spherical earth gravity and magnetic anomaly analysis by equivalent point source inversion: Earth Plan. Sci. Lett., **53**, 69–83.

von Frese, R. R. B., Ravat, D. N., Hinze, W. J., and McGue, C. A., 1988, Improved inversion of geopotential field anomalies for lithospheric investigations: Geophysics, **53**, 375–385.

## APPENDIX A

### EVALUATION OF INTEGRAL (11)

Consider the integral

$$I = \int_{-\infty}^{+\infty}\int_{-\infty}^{+\infty} g(\alpha - x_m, \beta - y_m, z_m - h) \cdot g(\alpha - x_j, \beta - y_j, z_j - h)\, d\alpha\, d\beta, \qquad \text{(A-1)}$$

for two arbitrary points $(x_m, y_m, z_m)$ and $(x_j, y_j, z_j)$, and $g(\alpha - x_m, \beta - y_m, z_m - h)$ given by

$$g(\alpha - x_m, \beta - y_m, z_m - h) = \frac{(z_m - h)}{[(\alpha - x_m)^2 + (\beta - y_m)^2 + (h - z_m)^2]^{3/2}}. \qquad \text{(A-2)}$$

This integral can be evaluated using the Fourier transform pair for point $(x_m, y_m, z_m)$

$$\frac{(z_m - h)}{[(\alpha - x_m)^2 + (\beta - y_m)^2 + (h - z_m)^2]^{3/2}} \leftrightarrow 2\pi e^{-(h - z_m)|K|} e^{-i(x_m k_x + y_m k_y)}, \qquad \text{(A-3)}$$

where

$$|K| = \sqrt{k_x^2 + k_y^2}, \qquad \text{(A-4)}$$

$i = \sqrt{-1}$, and the 2-D Parseval's theorem:

$$\int_{-\infty}^{+\infty}\int_{-\infty}^{+\infty} h_1(\alpha, \beta)\cdot h_2(\alpha, \beta)\, d\alpha\, d\beta$$

$$= \frac{1}{4\pi^2}\int_{-\infty}^{+\infty}\int_{-\infty}^{+\infty} H_1(-k_x, -k_y)\cdot H_2(k_x, k_y) dk_x\, dk_y \tag{A-5}$$

where $h_1$ and $h_2$ are Fourier transform pairs of $H_1$ and $H_2$, respectively.

Using the pair given in equations (A-3) and (A-5), the integral (A-1) can be written as

$$\int_{-\infty}^{+\infty}\int_{-\infty}^{+\infty} e^{-(h - z_m)|K|} e^{\imath(x_m k_x + y_m k_y)} \cdot e^{-(h - z_j)|K|} e^{-\imath(x_j k_x + y_j k_y)}\, dk_x\, dk_y. \tag{A-6}$$

By remembering that

$$\frac{1}{4\pi^2}\int_{-\infty}^{+\infty}\int_{-\infty}^{+\infty} 2\pi e^{-(2h - z_m - z_j)|K|} \cdot e^{-i[(x_j - x_m)k_x + (y_j - x_m)k_y]} \cdot e^{i(\alpha k_x + \beta k_y)} dk_x\, dk_y|_{(\alpha, \beta) = (0, 0)} \tag{A-7}$$

is an inverse Fourier transform, evaluated at the origin in the wavenumber domain and considering the Fourier transform pair given by equation (A-3), we have

$$I = f(x_j - x_m, y_j - y_m, 2h - z_j - z_m) = -2\pi g(x_j - x_m, y_j - y_m, 2h - z_j - z_m), \tag{A-8}$$

or

$$I = f(x_j - x_m, y_j - y_m, 2h - z_j - z_m) = -2\pi \frac{2h - z_j - z_m}{[(x_j - x_m)^2 + (y_j - y_m)^2 + (2h - z_j - z_m)^2]^{3/2}} \tag{A-9}$$

which, except for the constant $2\pi$, is the same expression as the Green's function for a point mass.